International Journal of Minerals, Metallurgy and Materials
Volume 21, Number 12, December 2014, Page 1215
DOI: 10.1007/s12613-014-1029-z

Microstructural evolution of Al–8.59Zn–2.00Mg–2.44Cu during homogenization

Wen-xiang Shu[1)], *Jun-cheng Liu*[1)], *Long-gang Hou*[1)], *Hua Cui*[2)], *Jun-tao Liu*[1,3)], *and Ji-shan Zhang*[1)]

1) State Key Laboratory for Advanced Metals and Materials, University of Science and Technology Beijing, Beijing 100083, China

2) School of Materials Science and Engineering, University of Science and Technology Beijing, Beijing 100083, China

3) State Key Laboratory for Fabrication and Processes of Nonferrous Metals, General Research Institute for Nonferrous Metals, Beijing 100088, China

(Received: 14 April 2014; revised: 28 July 2014; accepted: 3 September 2014)

Abstract: The microstructural evolution and phase transformations of a high-alloyed Al–Zn–Mg–Cu alloy (Al–8.59Zn–2.00Mg–2.44Cu, wt%) during homogenization were investigated. The results show that the as-cast microstructure mainly contains dendritic α(Al), non-equilibrium eutectics (α(Al) + $Mg(Zn,Al,Cu)_2$), and the θ (Al_2Cu) phase. Neither the T ($Al_2Mg_3Zn_3$) phase nor the S (Al_2CuMg) phase was found in the as-cast alloy. The calculated phase components according to the Scheil model are in agreement with experimental results. During homogenization at 460°C, all of the θ phase and most of the $Mg(Zn,Al,Cu)_2$ phase were dissolved, whereas a portion of the $Mg(Zn,Al,Cu)_2$ phase was transformed into the S phase. The type and amount of residual phases remaining after homogenization at 460°C for 168 h and by a two-step homogenization process conducted at 460°C for 24 h and 475°C for 24 h (460°C/24 h + 475°C/24 h) are in good accord with the calculated phase diagrams. It is concluded that the Al–8.59Zn–2.00Mg–2.44Cu alloy can be homogenized adequately under the 460°C/24 h + 475°C/24 h treatment.

Keywords: aluminum alloys; homogenization; microstructural evolution; phase composition; thermodynamic calculations

1. Introduction

High strength Al–Zn–Mg–Cu alloys, such as AA 7050, AA 7010, AA 7055, and the most recently developed AA 7085 Al alloys, are widely used as structural parts in the aeronautics industry owing to their high specific strength, high toughness, and good corrosion resistance [1–2]. To obtain a greater weight reduction for airframe structures, and to accommodate the challenge of composite materials, additional improvements in the properties of Al–Zn–Mg–Cu alloys, e.g., static strength, fatigue, damage tolerance, and corrosion resistance, are greatly desired [3].

As one of the major alloying elements in Al–Zn–Mg–Cu alloys, the element Zn has significant influence on the volume fraction of η′ and η strengthening phases as well as on the alloy's strength [4]. A feature of the newly registered Al–Zn–Mg–Cu alloys (e.g., AA 7136, AA 7056, and AA 7095) with high strength and toughness is their high Zn content, and these high-Zn alloys usually contain a high total solute content (Zn + Mg + Cu). However, it is typically difficult to fully homogenize high-alloyed Al–Zn–Mg–Cu alloys, and the undissolved coarse particles, e.g., Fe-rich, T, and S phases, can affect the hot workability and recrystallization behavior of Al–Zn–Mg–Cu alloys, which may result in a decrease of strength and toughness [5–7]. For a greater utilization of substantial alloying elements that are added, proper homogenization processes must be applied to decrease composition segregation and to dissolve soluble intermetallic phases as much as possible. Currently, both the phase component research and reference phase diagram are usually pertinent to low-Zn Al–Zn–Mg–Cu alloys [8–13], and less attention has been focused on the alloys with high Zn content [5,14–15]. Moreover, various phase components were observed in the as-cast or homogenized alloys with different compositions. For example, in the as-cast 7055 alloy, the $Mg(Zn,Al,Cu)_2$, T, S, and θ phases were found, and after homogenization at 450°C for 35 h, some T and S

Corresponding author: Long-gang Hou E-mail: lghou@skl.ustb.edu.cn

phases still remained [15]. In the as-cast 7050 alloy, the $Mg(Zn,Al,Cu)_2$, S, θ, Mg_2Si, Al_7Cu_2Fe, and $Al_{13}Fe_4$ phases were observed [16], whereas, for the as-cast 7150 alloy, only the $Mg(Zn,Al,Cu)_2$ and Al_7Cu_2Fe phases were found, and a phase transformation from the $Mg(Zn,Al,Cu)_2$ phase to the S phase was observed during homogenization [9].

We investigated the microstructural evolution and phase transformation of a high-alloyed Al–Zn–Mg–Cu alloy (Al–8.59Zn–2.00Mg–2.44Cu, wt%) during homogenization in the present study. The alloy considered is a typical high-Zn 7xxx alloy, which also has a high Zn/Mg ratio and a substantial total solute content (Zn + Mg + Cu), and these composition characteristics are thought to be beneficial for obtaining high strength and toughness. It is expected to develop a suitable homogenization process via understanding the dissolution of added alloying elements. In addition, related thermodynamic calculations were performed to provide a reference for alloy design and process optimization for Al–Zn–Mg–Cu alloys with a Zn content of around 8.5wt%.

2. Experimental

The Al–8.59Zn–2.00Mg–2.44Cu (wt%) alloy was designed and prepared with high purity Al (99.99%), Zn (99.99%), Mg (99.99%), and Al–50Cu, Al–10Zr, and Al–10Ti (wt%) master alloys. The original materials were melted in an electrical-resistance furnace and the melts were poured into a water-cooled steel mold, and the size of the ingot is about 210 mm × 120 mm × 100 mm. The content of impurity elements such as Fe and Si in the alloy was controlled to a concentration below 0.02wt%, which is beneficial for the improvement of mechanical properties and the utilization of added elements, and is also favorable for studying the distributions of the main alloying elements as well as their various influences on the solidification path. Specimens of 12 mm × 12 mm × 12 mm were cut from the quarter thickness position of the ingot. The specimens were heated at a 30°C/h heating rate to the homogenization temperature of 460°C and held for various times (12 h, 24 h, and 168 h), and then quenched in room temperature water to retain the high-temperature microstructures for analysis. In addition, a two-step homogenization process comprised of 460°C/24 h followed by 475°C/24 h (460°C/24 h + 475°C/24 h) was designed to eliminate the S phase effectively. The holding temperatures of the single and two-step homogenization processes for the as-cast alloy were chosen according to differential scanning calorimetry (DSC) results.

The characteristic temperatures of the different phase transformations of the present alloy were tested by DSC using a TA2910 differential scanning calorimeter at a 10°C/min heating rate from room temperature to 550°C. The DSC samples were 3 mm-diameter discs with a mass of about 10 mg, and a high purity aluminum disc of the same weight was also tested as a reference. The microstructures and phase components of the alloy in different states were analyzed by scanning electron microscope (SEM) (ZEISS LEO 1450) equipped with an energy dispersive X-ray spectroscopy (EDS) unit, and by X-ray diffraction (XRD) (Rigaku D_{MAX}-RB X-ray diffractometer; Cu K_α radiation; a working voltage of 40 kV; a step length of 0.02°; a scanning rate of 9°/min). The SEM specimens were polished without etching. Combining the above analyses, the microstructural evolution of the present alloy during homogenization was studied. The area fractions of coarse particles ($Mg(Zn,Al,Cu)_2$ and S phases) in the as-cast and homogenized samples were measured from the SEM images using the Image-Pro Plus image analysis software, and 15–20 images were captured at a magnification of 200 times and analyzed for relatively accurate area fraction estimates.

Phase diagram calculations were performed using the FactSage thermodynamic calculation software, which can be used for phase equilibrium calculations of complicated multi-component aluminum alloys, and is helpful for researching and developing new aluminum alloys. In addition, the mole fractions of the constituent phases according to the Scheil model were calculated using the Pandat software. Thermodynamic calculations in this work were compared with experimental results, and consistency was found between them.

3. Results

3.1. Microstructure and phase component of the as-cast alloy

In the as-cast Al–8.59Zn–2.00Mg–2.44Cu alloy, a typical aluminum dendritic network appears, as shown in Fig. 1(a), as well as coarse, continuous non-equilibrium eutectic microstructures along grain boundaries, and some scattered particles are also observed in the grains. Moreover, a lamellar eutectic structure and a discrete particle can be seen clearly in Fig. 1(b). Table 1 presents the result of the quantitative EDS analyses of positions marked in Fig. 1(b), and it shows that the composition of the white intermetallic phase (positions A and C) is close to stoichiometric $Mg(Zn,Al,Cu)_2$, and it is corroborated by XRD patterns given in Fig. 2(a). The composition of position B was determined via defocused beam EDS analysis, which yields an

average composition of (α(Al) + $Mg(Zn,Al,Cu)_2$) eutectics. The content of solute atoms in these eutectics is approximately half of that in the $Mg(Zn,Al,Cu)_2$ phase because the α(Al) matrix contributes to a higher Al content in the compounds when analyzed according to the energy spectrum [14]. The composition of the grayish phase (position D) is close to the θ phase, although no clear diffraction peak in Fig. 2(a) is attributable to this phase due to its small concentration. The DSC curve of the as-cast alloy is shown in Fig. 2(b), and two endothermic peaks in the temperature range 400–550°C are observed: peak 1 around 467°C and peak 2 around 478°C. It is known that non-equilibrium eutectics can be melted during the DSC heating process, and the endothermic reaction indicated by peak 2 can be attributed to the melting of these eutectics containing the $Mg(Zn,Al,Cu)_2$ phase [9]. More intrinsically, this endothermic reaction can be regarded as the melting of the $Mg(Zn,Al,Cu)_2$ phase. According to SEM observation and thermodynamic calculation results hereinafter, the endothermic reaction indicated at peak 1 can be attributed to the melting of the θ phase. To our knowledge, peak 1 has only been reported by Mukhopadhyay [17] until now, but the related reaction has not been discussed. Moreover, our recent studies on a series of Al–8.5Zn–*x*Mg–*y*Cu alloys (wt%) indicate that the θ phase would exist in the as-cast alloys for high-Zn, low/middle-Mg, and high-Cu Al–Zn–Mg–Cu alloys. Analysis of the Al_7Cu_2Fe or Mg_2Si phase is difficult owing to the low content of Fe and Si in the alloy under consideration.

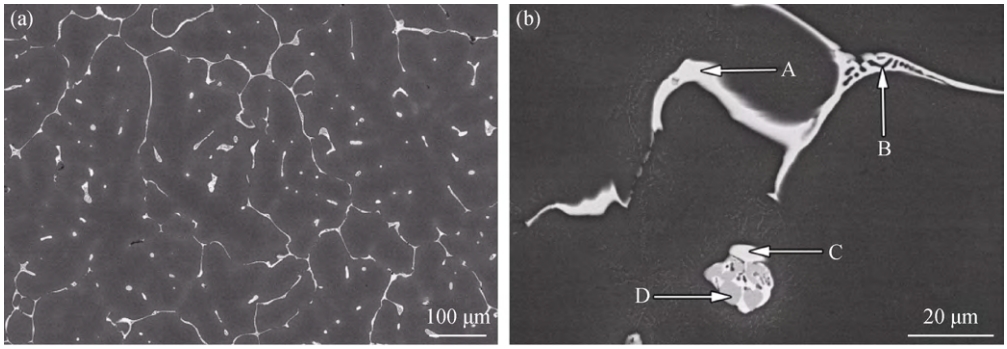

Fig. 1. SEM images with low (a) and high (b) magnification of the as-cast Al–8.59Zn–2.00Mg–2.44Cu alloy.

Table 1. EDS elemental analyses of positions marked in Fig. 1(b) wt%

Position	Mg	Al	Cu	Zn
A	32.91	26.21	16.11	24.77
B	15.87	60.20	10.06	13.87
C	32.62	22.40	17.44	27.53
D	1.38	67.15	29.73	1.74

3.2. Microstructures and phase components of the homogenized alloys

Figs. 3(a), 3(b), 3(c), and 3(d) present microstructure images of the alloy after different homogenization procedures of 460°C/12 h, 460°C/24 h, 460°C/168 h, and 460°C/24 h + 475°C/24 h, respectively, and the result of the quantitative EDS analyses of positions marked in Fig. 3 is shown in Table 2. After homogenization at 460°C for 12 h,

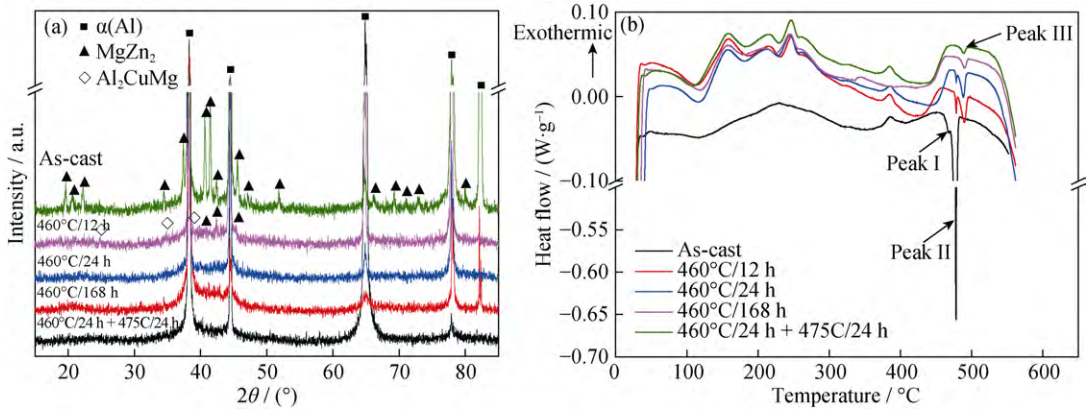

Fig. 2. XRD patterns (a) and DSC curves (b) of the as-cast and homogenized Al–8.59Zn–2.00Mg–2.44Cu alloy.

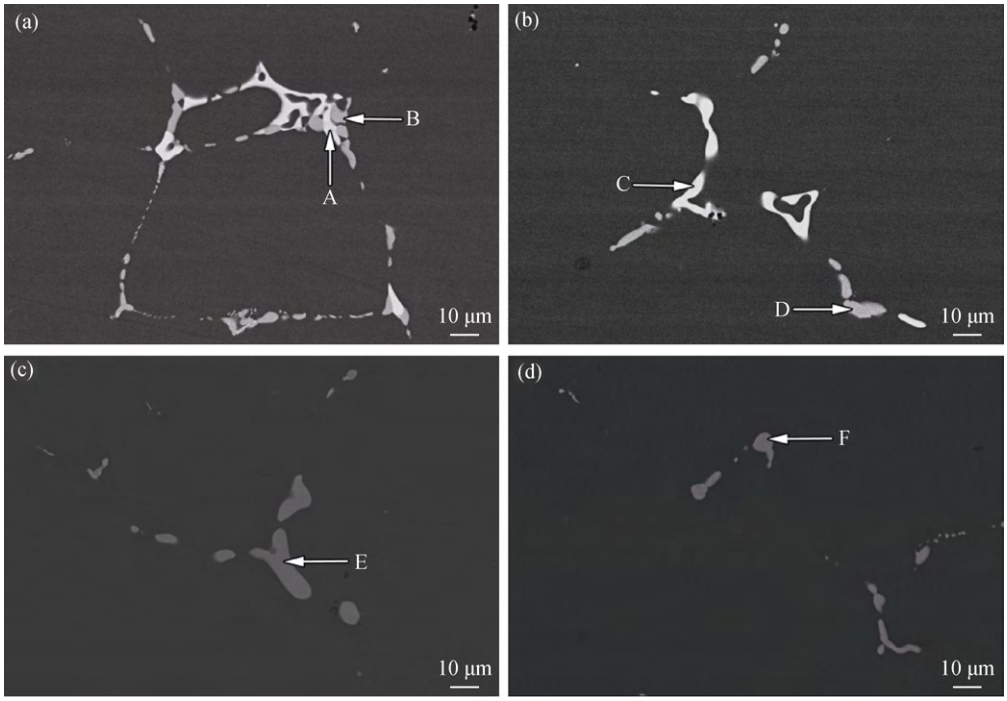

Fig. 3. SEM images of the homogenized Al–8.59Zn–2.00Mg–2.44Cu alloy: (a) 460°C/12 h; (b) 460°C/24 h; (c) 460°C/168 h; (d) 460°C/24 h + 475°C/24 h.

Table 2. EDS elemental analyses of positions marked in Fig. 3

wt%

Position	Mg	Al	Cu	Zn
A	31.98	38.19	13.58	16.25
B	24.31	55.99	17.77	1.94
C	28.82	39.47	14.02	17.69
D	23.75	55.10	19.54	1.61
E	24.86	50.61	22.38	2.14
F	24.38	50.78	22.79	2.05

the amount of non-equilibrium eutectics along grain boundaries is decreased, and scattered particles in the grains are dissolved (Fig. 3(a)); however, a new gray phase (position B) develops with a composition close to stoichiometric Al_2CuMg. Furthermore, gray particles given in positions such as B, D, E, and F in Fig. 3 can be identified as the S phase by XRD and DSC results. By increasing the homogenization time to 24 h (at 460°C), the eutectic structures are observed to disappear with only a few isolated $Mg(Zn,Al,Cu)_2$ and S phases remaining at grain boundaries (Fig. 3(b)). Fig. 3(c) shows that the $Mg(Zn,Al,Cu)_2$ phase has completely disappeared after conducting homogenization for 168 h at 460°C, although some S phase particles remain. With two-step homogenization (460°C/24 h + 475°C/24 h), both the size and total area fraction of the residual S phase particles appear to be smaller (Fig. 3(d)). The quantitative analysis results indicating the area fractions of various phases in the Al–8.59Zn–2.00Mg–2.44Cu alloy after conducting the various homogenization procedures are shown in Fig. 4(a).

The XRD patterns and DSC curves of the alloy after various homogenization procedures are shown in Fig. 2. The XRD and DSC results are consistent with SEM observations. The corresponding peak temperature T_P and reaction heat ΔH_R associated with phase dissolution calculated from the DSC curves are listed in Table 3. According to calculated parameters in Table 3, after homogenization at 460°C for 12 h, peak 1 disappears, and peak 2 is greatly weakened while a new endothermic peak (peak 3 around 490°C) indicating the S phase dissolution emerges [18]. Therefore, it can be inferred that the θ phase and most of the $Mg(Zn,Al,Cu)_2$ phase dissolve while a new S phase forms during homogenization. Also, it can be found that the amount of $Mg(Zn,Al,Cu)_2$ decreases during homogenization until its complete dissolution after holding for 168 h at 460°C. The amount of the S phase also decreases with further homogenization, although it remains even after the two-step homogenization. In general, the fluctuation of DSC curves is indicative of solid state reactions accompanying heating/cooling, and the ΔH_R associated with an endothermic reaction is proportional to the volume fraction of the dissolved phases [19]. The evolutions of the ΔH_R associated with the dissolution of the $Mg(Zn,Al,Cu)_2$ and S phases are shown in Fig. 4(b), which

represent similar variational trends of the amounts of the $Mg(Zn,Al,Cu)_2$ and S phases as those shown in Fig. 4(a). Moreover, the stable values of the peak temperature T_P in Table 3 can reflect the relative stability of the composition of these phases, and this is consistent with EDS results given in Table 1 and Table 2.

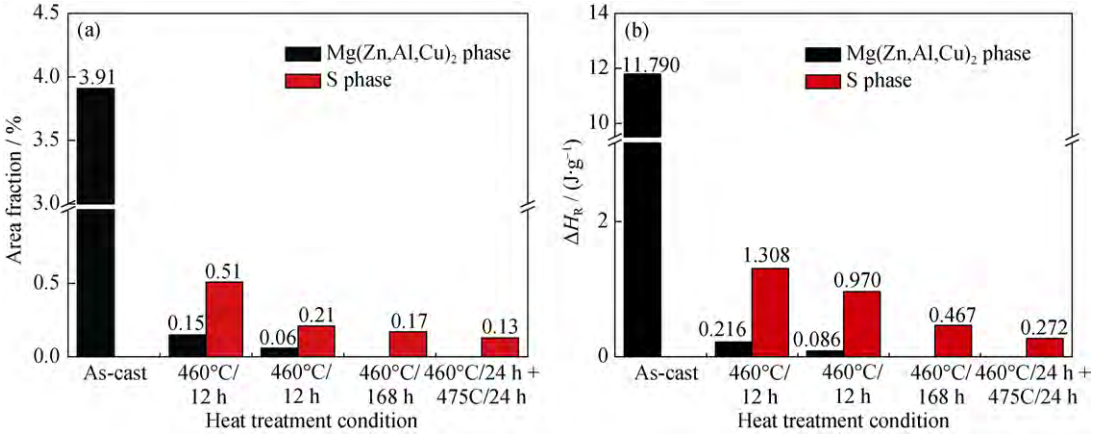

Fig. 4. Quantitative analysis results reflecting the concentrations of various phases in the Al–8.59Zn–2.00Mg–2.44Cu alloy before and after homogenization (analysis of the θ phase is not included due to its small concentration): (a) Area fraction of the $Mg(Zn,Al,Cu)_2$ and S phases; (b) ΔH_R associated with the dissolution of the $Mg(Zn,Al,Cu)_2$ and S phases.

Table 3. Peak temperature T_P and reaction heat ΔH_R calculated from the DSC curves of the as-cast and homogenized Al–8.59Zn–2.00Mg–2.44Cu alloy

Heat treatment	Peak 1		Peak 2		Peak 3	
	T_P / °C	ΔH_R / (J·g^{-1})	T_P / °C	ΔH_R / (J·g^{-1})	T_P / °C	ΔH_R / (J·g^{-1})
As-cast	467.3	0.135	478.2	11.790	—	—
460°C/12 h	—	—	478.5	0.216	490.06	1.308
460°C/24 h	—	—	478.6	0.086	488.57	0.970
460°C/168 h	—	—	—	—	490.06	0.467
460°C/24 h + 475°C/24 h	—	—	—	—	489.20	0.272

4. Discussion

Numerous studies have been conducted to evaluate the phase components of as-cast Al–Zn–Mg–Cu alloys, but different results were obtained. Various combinations of the $Mg(Zn,Al,Cu)_2$, T, S, and θ phases were regarded as the main intermetallic phases in the as-cast alloys [9,15–16, 20–21], and some differences in the phase components are found between the present research and the earlier literature. The most frequently observed phase of the as-cast 7xxx alloys has routinely been the quaternary Al–Zn–Mg–Cu phase that always exists in the non-equilibrium eutectics. This quaternary phase has been confirmed to have the same crystal structure as that of the $MgZn_2$ phase [21–22], and this quaternary phase is usually referred to as $Mg(Zn,Al,Cu)_2$. In some literatures, the partial quaternary Al–Zn–Mg–Cu phase was regarded as the T phase according to EDS results [15,23]; however, as is well known, the composition of the T phase with a substantial component of dissolved Cu would be variable, and EDS results alone cannot reliably identify the quaternary phase as the T phase. The composition of the present $Mg(Zn,Al,Cu)_2$ phase is similar to that of the T phase given previously [15,23]. Phase equilibrium calculations for the Al–5.9Zn–2.5Mg–1.9Cu alloy show that the amount of the T phase present can be reduced with increasing Zn content or decreasing Mg content [4], and in the Al–6.1Zn–1.9Mg–1.9Cu alloy (with a Zn/Mg weight ratio of 3.2), no T phase appeared in the temperature range 100–500°C [4]. In addition, no S phase was observed in the as-cast alloy in the present study, although the S phase has been observed in the alloys with similar Cu content [15–16]. Also, the θ phase is not always present in as-cast Al–Zn–Mg–Cu alloys, and according to related research [15] and our recent studies, this phase will tend to form in Al–Zn–Mg–Cu alloys with a high Zn, low/middle Mg, and high Cu content. The mole fractions of constituent phases in Al–8.50Zn–2.00Mg–2.50Cu–0.11Zr (wt%) according to the Scheil model have been calculated, and the results are

shown in Fig. 5. The calculated phase components of the as-cast alloy are in agreement with experimental results.

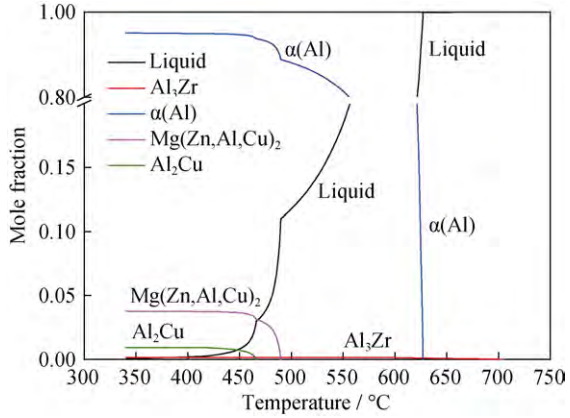

Fig. 5. Plots of the mole fraction of calculated phases vs. temperature for the Al–8.50Zn–2.00Mg–2.50Cu–0.11Zr alloy according to the Scheil model.

During homogenization at 460°C, the $Mg(Zn,Al,Cu)_2$ and θ phases are dissolved gradually, meanwhile, the S phase content arises in locations previously occupied by the $Mg(Zn,Al,Cu)_2$ phase. This implies that the $Mg(Zn,Al,Cu)_2$ phase may transform to the S phase, which is consistent with the research results of low-Zn Al–Zn–Mg–Cu alloys [8–9]. We performed thermodynamic analysis of phase transformations in the Al–8.59Zn–2.00Mg–2.44Cu alloy during homogenization using phase diagram calculations, and the calculated isothermal sections of the Al–Zn–Mg–Cu system for 8.5wt% Zn at 460°C and 475°C are shown in Figs. 6(a) and 6(b), respectively. Fig. 6(a) indicates that only α(Al) and S phases exist at 460°C when the alloy finally reaches its equilibrium state. In other words, when the system is at 460°C, the S phase has the lowest Gibbs free energy, indicating that the $Mg(Zn,Al,Cu)_2$ phase with a higher free energy is unstable at this temperature. Therefore, during homogenization at 460°C, the $Mg(Zn,Al,Cu)_2$ phase is expected to be dissolved into the α(Al) matrix and also spontaneously transforms to the S phase. These phase transformations are diffusion-dependent processes, and the diffusion coefficient of Cu is much lower than those of Mg and Zn at 460°C; therefore, the amount of the S phase component can be expected to reach a peak value within the initial homogenization period (i.e., ≤ 12 h) and then begins to gradually decrease to its equilibrium content.

Additionally, it can be observed that the experimental results agree well with calculated phase diagrams shown in Fig. 6. For example, after a holding time of 168 h at 460°C, all $Mg(Zn,Al,Cu)_2$ phase disappeared, but some S phase still remained, and a very small amount of S phase existed after the two-step homogenization. The present alloy has a high Cu content and middle-level Mg content, and its composition is in the (α + S) field at 475°C, closing to the solvus line in the calculated phase diagram. As a result, the Al–8.59Zn–2.00Mg–2.44Cu alloy can be well homogenized with the two-step homogenization treatment (460°C/24 h + 475°C/24 h).

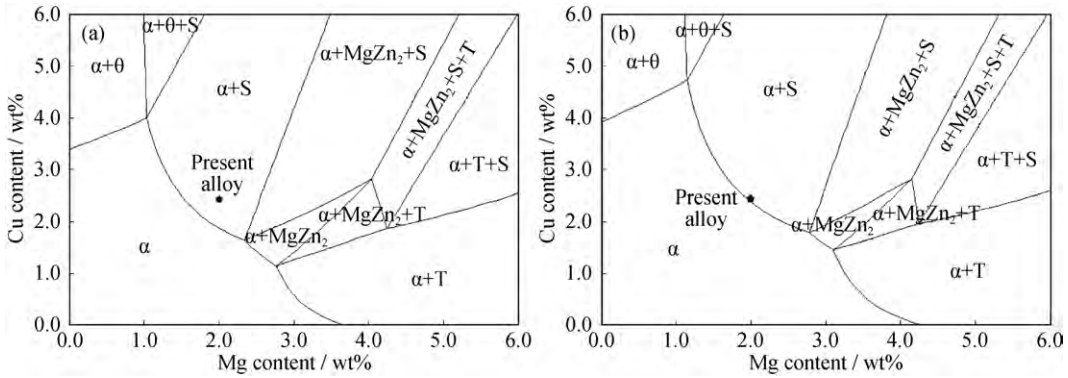

Fig. 6. Isothermal sections of the Al–Zn–Mg–Cu phase diagram for 8.5wt% Zn: (a) at 460°C; (b) at 475°C.

5. Conclusions

(1) The as-cast microstructure of the Al–8.59Zn–2.00Mg–2.44Cu alloy mainly contains dendritic α(Al), non-equilibrium eutectics (α(Al) + $Mg(Zn,Al,Cu)_2$) and the θ phase, and neither the T phase nor S phase is found. The calculated phase components according to the Scheil model are in agreement with experimental results.

(2) During homogenization at 460°C, all of the θ phase and most of the $Mg(Zn,Al,Cu)_2$ phase are dissolved, whereas some of the $Mg(Zn,Al,Cu)_2$ phase is transformed into the S phase.

(3) The type and amount of residual phases after homogenizations by the 460°C/168 h and 460°C/24 h + 475°C/24 h procedures are in good accord with calculated phase diagrams.

(4) The Al–8.59Zn–2.00Mg–2.44Cu alloy can be homogenized adequately by the 460°C/24 h + 475°C/24 h treatment.

Acknowledgements

This work was supported by the Fundamental Research Funds for the Central Universities of China (No. FRF-TD-12-001) and the Beijing Laboratory of Modern Traffic Metal Materials and Processing Technology. The authors additionally wish to thank CompuTherm LLC for their support in the solidification simulation work.

References

[1] E.A. Starke and J.T. Staley, Application of modern aluminum alloys to aircraft, *Prog. Aerosp. Sci.*, 32(1996), No. 2-3, p. 131.

[2] J. Liu, Advanced aluminium and hybrid aerostructures for future aircraft, *Mater. Sci. Forum*, 519-521(2006), p. 1233.

[3] A.S. Warren, Developments and challenges for aluminum: a Boeing perspective, *Mater. Forum*, 28(2004), p. 24.

[4] J.J. Yu and X.M. Li, Modelling of the precipitated phases and properties of Al–Zn–Mg–Cu alloys, *J. Phase Equilib. Diffus.*, 32(2011), No. 4, p. 350.

[5] W.B. Li, Q.L. Pan, Y.P. Xiao, Y.B. He, and X.Y. Liu, Microstructural evolution of ultra-high strength Al–Zn–Cu–Mg–Zr alloy containing Sc during homogenization, *Trans. Nonferrous Met. Soc. China*, 21(2011), No. 10, p. 2127.

[6] J.H. Mulherin and H. Rosenthal, Influence of nonequilibrium second-phase particles formed during solidification upon the mechanical behavior of an aluminum alloy, *Metall. Trans.*, 2(1971), p. 427.

[7] S.T. Lim, Y.Y. Lee, and I.S. Eun, Dilute alloy designs of 7xxx aluminum alloys for thick forging applications, *Mater. Sci. Forum*, 475-479(2005), p. 369.

[8] Y.L. Deng, L. Wan, L.H. Wu, Y.Y. Zhang, and X.M. Zhang, Microstructural evolution of Al–Zn–Mg–Cu alloy during homogenization, *J. Mater. Sci.*, 46(2011), No. 4, p. 875.

[9] X.G. Fan, D.M. Jiang, Q.C. Meng, N.K. Li, and Z.X. Sun, Evolution of intermetallic phases of Al–Zn–Mg–Cu alloy during heat treatment, *Trans. Nonferrous Met. Soc. China*, 16(2006), Suppl. 3, p. 1247.

[10] Y. Deng, Z.M. Yin, and F.G. Cong, Intermetallic phase evolution of 7050 aluminum alloy during homogenization, *Intermetallics*, 26(2012), p. 114.

[11] X.M. Li and M.J. Starink, The effect of compositional variations on the characteristics of coarse intermetallic particles in overaged 7xxx Al alloys, *Mater. Sci. Technol.*, 17(2001), p.1324.

[12] V. Raghavan, Al–Cu–Mg–Zn (aluminum–copper–magnesium–zinc), *J. Phase Equilib. Diffus.*, 28(2007), No. 2, p. 211.

[13] N.A. Belov, D.G. Eskin, and A.A. Aksenov, *Multicomponent Phase Diagrams*: *Applications for Commercial Aluminum Alloys*, Elsevier, Amsterdam, 2005, p. 212.

[14] Y.X. Li, P. Li, G. Zhao, X.T. Liu, and J.Z. Cui, The constituents in Al–10Zn–2.5Mg–2.5Cu aluminum alloy, *Mater. Sci. Eng. A*, 397(2005), No. 1-2, p. 204.

[15] C. Mondal and A.K. Mukhopadhyay, On the nature of T($Al_2Mg_3Zn_3$) and S(Al_2CuMg) phases present in as-cast and annealed 7055 aluminum alloy, *Mater. Sci. Eng. A*, 391(2005), No. 1-2, p. 367.

[16] F.Y. Xie, X.Y. Yan, L. Ding, F. Zhang, S.L. Chen, M.G. Chu, and Y.A. Chang, A study of microstructure and microsegregation of aluminum 7050 alloy, *Mater. Sci. Eng. A*, 355(2003), No. 1-2, p. 144.

[17] A.K. Mukhopadhyay, Selection and design principles of wrought aluminium alloys for structural applications, *Mater. Sci. Forum*, 710(2012), p. 50.

[18] D.K. Xu, P.A. Rometsch, and N. Birbilis, Improved solution treatment for an as-rolled Al–Zn–Mg–Cu alloy: Part I. Characterisation of constituent particles and overheating, *Mater. Sci. Eng. A*, 534(2012), p. 234.

[19] D. Richard and P.N. Adler, Calorimetric studies of 7000 series aluminum alloys: I. Matrix precipitate characterization of 7075, *Metall. Trans. A*, 8(1977), No. 7, p. 1177.

[20] K.H. Chen, H.W. Liu, Z. Zhang, S. Li, and R.I. Todd, The improvement of constituent dissolution and mechanical properties of 7055 aluminum alloy by stepped heat treatments, *J. Mater. Process. Technol.*, 142(2003), No. 1, p. 190.

[21] F.H. Gao, G. Zhao, W.M. Bian, and N. Tian, TEM *in-situ* investigation on non-equilibrium eutectics in semicontinuous casting ingot of Al–6.2Zn–2.3Mg–2.3Cu super-high strength aluminum alloy, *Mater. Sci. Forum*, 638-642(2010), p. 384.

[22] X.L. Han, B.Q. Xiong, Y.A. Zhang, Z.H. Li, B.H. Zhu, and F. Wang, Microstructure of as-cast and as-homogenized 7150 aluminum alloy, *Trans. Mater. Heat Treat.*, 31(2010), No. 11, p. 104.

[23] H. Zhong, Y. Han, Z.Z. Deng, and Y.K. Le, Study on the microstructure of as-cast and homogenized 7150 aluminum alloy, *Heat Treat. Met.*, 33(2008), No. 4, p. 36.